INSTITUTE OF PHYSICS PUBLISHING and INTERNATIONAL ATOMIC ENERGY AGENCY NUCLEAR FUSION

Nucl. Fusion **45** (2005) 1213–1223 doi:10.1088/0029-5515/45/11/001

Small ELM regimes with good confinement on JET and comparison to those on ASDEX Upgrade, Alcator C-mod and JT-60U

J. Stober[1], P.J. Lomas[2], G. Saibene[3], Y. Andrew[2], P. Belo[4], G.D. Conway[1], A. Herrmann[1], L.D. Horton[1], M. Kempenaars[5], H.-R. Koslowski[6], A. Loarte[3], G.P. Maddison[2], M. Maraschek[1], D.C. McDonald[2], A.G. Meigs[2], P. Monier-Garbet[7], D.A. Mossessian[8], M.F.F. Nave[4], N. Oyama[9], V. Parail[2], Ch.P. Perez[6], F. Rimini[7], R. Sartori[3], A.C.C. Sips[1], P.R. Thomas[7], Contributors to the EFDA-JET workprogramme[a] and the ASDEX Upgrade Team

[1] MPI für Plasmaphysik, EURATOM Association, D-85748 Garching, Germany
[2] Euratom/UKAEA Association, Culham Science Centre, Abingdon, OX14 3DB, UK
[3] EFDA Close Support Unit (Garching), 2 Boltzmannstrasse, Garching, Germany
[4] Associação EURATOM/IST, Centro de Fusão Nuclear, 1049-001 Lisbon, Portugal
[5] FOM-Rijnhuizen, Association Euratom-FOM, TEC, PO Box 1207, Nieuwegein, The Netherlands
[6] Forschungszentrum Jülich GmbH, Institut fur Plasmaphysik, EURATOM Association, Trilateral Euregio Cluster, 52425 Jülich, Germany
[7] Association Euratom-CEA, Cadarache, F-13108 St Paul-lez-Durance, France
[8] Massachusetts Institute of Technology Cambridge, MA, USA
[9] JAERI, Naka Fusion Research Establishment, Naka-machi, Naka-gun, Ibaraki-ken, 311-01, Japan

Received 10 December 2004, accepted for publication 14 June 2005
Published 17 October 2005
Online at stacks.iop.org/NF/45/1213

Abstract
Since it is uncertain if ITER operation is compatible with type-I edge localized modes (ELMs), the study of alternative ELM regimes is an urgent issue. This paper reports on experiments on JET aiming to find scenarios with small ELMs and good confinement, such as the type-II ELMs in ASDEX Upgrade, the enhanced D-alpha H-mode in Alcator C-mod or the grassy ELMs in JT-60U. The study includes shape variations, especially the closeness to a double-null configuration, variations of q_{95}, density and beta poloidal. H-mode pedestals without type-I ELMs have been observed only at the lowest currents ($\leqslant$1.2 MA), showing similarities to the observations in the devices mentioned above. These are discussed in detail on the basis of edge fluctuation analysis. For higher currents, only the mixed type-I/II scenario is observed. Although the increased inter-ELM transport reduces the type-I ELM frequency, a single type-I ELM is not significantly reduced in size. Obviously, these results do question the accessibility of such small ELM scenarios on ITER, except perhaps the high beta-poloidal scenario at higher q_{95}, which could not be tested at higher currents at JET due to limitations in heating power.

PACS numbers: 52.35.Py, 52.55.Fe, 52.55.Tn

(Some figures in this article are in colour only in the electronic version)

1. Introduction

Estimates of the amplitude of edge localized modes (ELMs) for the planned international test reactor ITER indicate that

[a] See the appendix of Pamela J. *et al* 2004 *Proc. 20th Int. Conf. on Fusion Energy 2004 (Vilamoura, 2004)* (Vienna: IAEA).

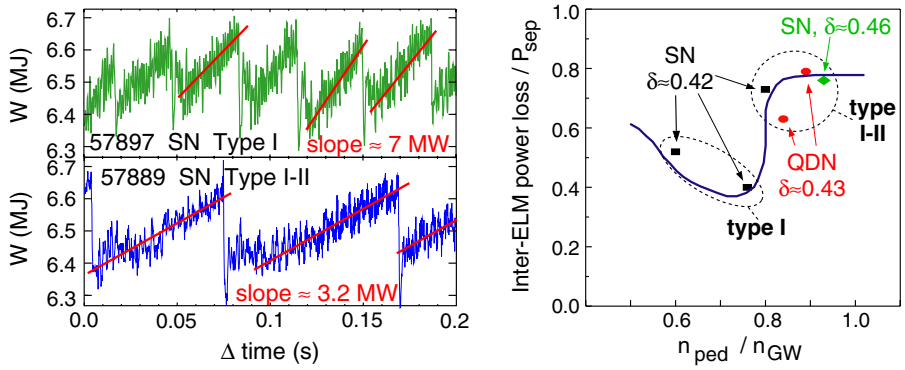

Figure 1. Mixed type-I/II H-modes in JET, $I_p = 2.5$ MA. Left: time evolution of the stored energy for two discharges with the most frequently used HT3-configuration ($q_{95} = 3.5$). The discharges have similar control parameters except gas puff. Pure type-I ELMs are observed with moderate gas puff (top, $n_{ped}/n_{GW} \approx 0.6$), mixed type-I/II ELMs are observed with strong gas puff (bottom, $n_{ped}/n_{GW} \approx 0.8$). The difference of the slopes of the inter-ELM energy-rise indicates a change in the inter-ELM energy confinement, i.e. increased inter-ELM losses during mixed type-I/II phases. Right: inter-ELM contribution to the average power flux across the separatrix ($P_{heat} - P_{rad,bulk}$). The black (blue) curve sketches the behaviour for the HT3-configuration ($q_{95} = 3.5$, black squares) to compare with the behaviour of other configurations ('ITER-like': green, QDN: red, both $q_{95} = 3.0$).

the peak power flux due to the expected type-I ELMs could severely limit the divertor lifetime for the standard $Q = 10$ (i.e. $P_{fus} = 10 \times P_{in}$) scenario at $q_{95} = 3$. The divertor lifetime could be as low as a few hundred discharges, although this depends strongly on the physics assumptions [1]. To be prepared for the worst case, techniques for ELM mitigation/control are being developed. This contribution reports on efforts to establish in the world's largest operational tokamak JET regimes with smaller (or no) ELMs and sufficient particle exhaust but nevertheless good H-mode energy confinement. The latter means that the ratio of the experimental energy confinement time τ_E to the scaled energy confinement time $\tau_{E,scal}$ according to the actual ITER scaling IPB98(y, 2) [2] should be close to unity. This ratio is usually referred to as H-factor H98(y, 2). The experiments described in the following are based on strategies derived from successful experiments on other devices, i.e. type-II ELMs on ASDEX Upgrade [3,4], grassy ELMs on JT-60U [5,6] and the 'Enhanced D-Alpha'(EDA) H-Mode on Alcator C-mod [7,8]. The Quiescent H-mode (QH) on DIII-D and ASDEX Upgrade has also been attempted in JET and is reported in a separate contribution [9].

As a starting point for these small ELM studies, the JET mixed type-I/II regime was chosen [10]. In these H-modes, increased edge transport between type-I ELMs is observed in high-triangularity (high-δ) equilibria at high density (>80% of the Greenwald density n_{GW}), up to a plasma current of 3 MA, the latter limited only by the available additional heating power [11]. Due to some similarities in the divertor-D_α traces and the observed increase in magnetic activity and power-flux across the separatrix between ELMs these phases were called mixed type-I/II phases, in analogy to similar observations on other machines. Figure 1 illustrates the effect of the mixed type-I/II ELMs on the power-flux across the separatrix due to ELMs and in between ELMs. The slopes in the left part of the figure indicate that for these two discharges with almost identical parameters, the inter-ELM transport in the mixed type-I/II phase is significantly higher than in the pure type-I phase (less transport leads to faster energy rise). The right part of the figure quantifies this for several phases and varying shape (as will be discussed in the next section). It shows that during these mixed type-I/II phases the inter-ELM power-flux can double from 40% (as observed in pure type-I ELM phases at slightly lower density) to 80% of the time-averaged power crossing the separatrix. But a comparison of the drops in the stored energy due to type-I ELMs in the upper and lower curve of the left part of the figure also shows that the type-I ELMs in the mixed type-I/II phase, which eject the remaining 20% of power, are similar in size to those observed in the pure type-I ELM phases at slightly lower densities. For these conditions we find $\Delta W \approx 150$–200 kJ and $\Delta W/W \approx 3\%$. For a more detailed discussion of ELM sizes in mixed type-I/II ELMy phase see [12]. It was reported in [13] that the enhanced inter-ELM transport is related to an increase in the strength of broadband MHD modes moving in the direction of the electron diamagnetic drift with frequencies between 10 and 40 kHz, which are called at JET washboard-modes (WB) [14]. In the same frequency range one finds enhanced density fluctuations close to the pedestal top with the far-infrared-interferometer [12]. In contrast to the type-II ELMs of ASDEX Upgrade, no high-frequent irregular, bursty events in the type-II phases in between type-I ELMs were found at JET [10, 12, 13]. Only recently, at the lowest plasma currents, i.e. $I_p = 1.1$ MA, smaller bursts in between the bigger ones have been found in magnetic and edge-density signals (figure 2). This indicates that the burstyness of the additional inter-ELM transport is not necessarily a good criterion to differentiate between small ELM types, but does itself depend on the actual pedestal parameters.

As explained above, the main drawback of the mixed type-I/II phase at JET are the remaining type-I ELMs, which still are a potential danger for the divertor of a future reactor. Therefore, additional efforts to further increase the inter-ELM transport on JET were undertaken and are described in the following sections. As these were stimulated by successful scenarios on other devices, this paper focuses on the inter-machine comparision of the results. Further detailed analysis of the JET results is found in [12, 15, 16]. Section 2

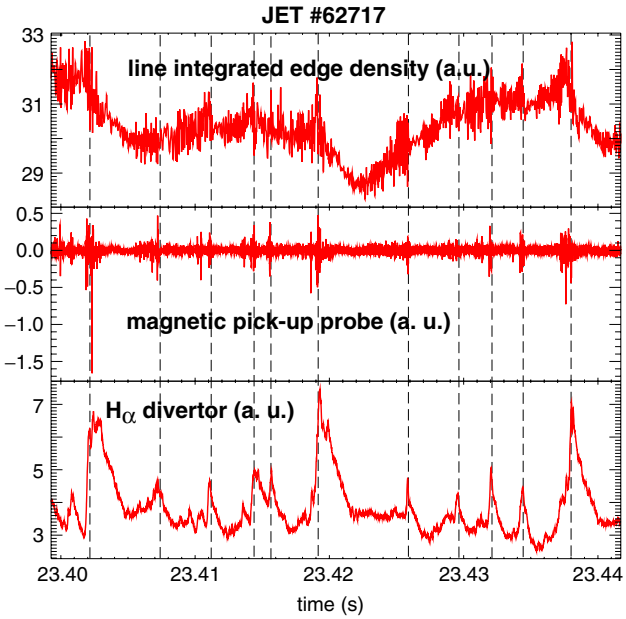

Figure 2. JET pulse 62717, high delta configuration (HT3) at 1.1 MA, 1.2 T, $q_{95} = 3.5$. Bottom: divertor H_α showing small bursts between type-I ELMs, which all show up in a magnetic signal from the outer midplane (middle). Top: line integrated edge density from a vertical interferometer channel tangential just inside the H-mode pedestal at the outer midplane. About half of the small bursts present in the lower time traces correlate with a drop of edge density.

describes how the mixed I/II regime reacts to increasing edge safety factor q_{95} and the closeness to a double null (DN) configuration, which have been identified as helpful on other devices. Section 3 describes the attempts to match in JET the EDA H-mode of Alcator C-mod and the type-II ELMy H-mode of ASDEX Upgrade with dimensionless identical plasmas to facilitate a scenario transfer. Section 4 reports on attempts to obtain the high β_{pol}-scheme on JET and ASDEX Upgrade, which is the basis for the grassy ELM operation in JT-60U.

2. Effect of DN and increased q_{95} on the JET mixed type-I/II ELM regime

The results of the ASDEX Upgrade type-II ELMs showed that a quasi-DN (QDN) configuration is an essential ingredient for that regime [3]. Therefore an single-null(SN)-configuration of JET which shows the mixed type-I/II regime was modified to be close to DN and still compatible with operation at 2.5 MA plasma current. The right part of figure 1 shows that the contribution of inter-ELM losses in the mixed type-I/II phases is similar for the SN and QDN shapes. In fact the confinement was often decreasing by up to 10% when approaching QDN, but it cannot be ruled out that this is due to insufficient conditioning of the upper divertor, which is only rarely used.

Both for SN and for QDN configurations q_{95} has been increased, following the experience from other devices, in which increased inter-ELM losses are observed only above a threshold in q_{95}. For EDA-H-mode on Alcator C-mod and pure type-II ELMs on ASDEX Upgrade $q_{95} > 3.5$ is found and for JT-60U the threshold value of q_{95} for pure grassy ELMs is

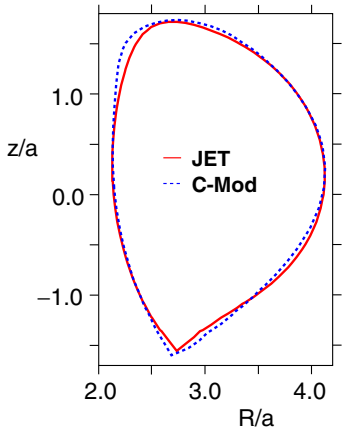

Figure 3. Scaled shapes used for the JET/Alcator C-mod pedestal identity experiments. The JET shape is very close to the HT3 high delta shape, used for the experiments at higher current as described in section 2.

between 4 and 6. In JET, an increase of q_{95} from 3 to 4 or, in a different configuration, from 3.6 to 4.7 led to a significant decrease (20%) of the pedestal density for the same level of gas puff, combined with an increased ELM frequency. Starting from an anchor point at $I_{\mathrm{p}} = 2.5$ MA and $B_{\mathrm{t}} = 2.7$ T, similar results have been obtained either by raising the magnetic field or by lowering the plasma current. With increased gas puff the density can be recovered, but only at reduced energy confinement and very high frequent ELMs; probably type-III. This means that a regime with $\mathrm{H98}(y, 2) \approx 1$, $q_{95} > 4$ and $n_{\mathrm{ped}} > 0.8 \times n_{\mathrm{GW}}$ has not been achieved at JET with any ELM type at plasma currents above 2 MA. There appears to be a significant dependence of particle confinement on q_{95}, specifically between ELMs [12], but the reasons for this are still unclear.

3. Dimensionless identity with small ELM regimes on Alcator C-mod and ASDEX Upgrade

A possible way to analyse the failure to obtain pure small ELM phases in JET at plasma currents above 2 MA are dimensionless identity experiments at low plasma current matching the respective plasmas in smaller machines. As shown by [17] the dimensionless parameters which govern the dimensionless equations for the fully ionized plasma are $\rho^*, \nu^*, \beta, q_{95}$, and of course the geometry, i.e. ϵ and the poloidal cross section (explicitly excluding effects on the scale of the Debye length, which would require additional dimensionless parameters). The constraint that $\rho^*, \nu^*, \beta, q_{95}$ have to be constant leads to a unique size scaling for the dimensional parameters. As a consequence, the smaller machine has to operate at the upper bound of its operational parameters whereas the larger machine (here, JET) has to operate at the lower bound, well below its design values. Since $B_{\mathrm{t}} \cdot \tau_E$ is an invariant of the scaling [18], all frequencies described by the plasma equations are expected to scale with the minor radius a as $f \propto 1/\tau \propto B \propto a^{-1.25}$, using $B \propto a^{-1.25}$ from [17]. For two machines with minor radii a_1, a_2 it follows $f_1/f_2 = (a_2/a_1)^{1.25}$. This holds, for example, for dimensionless identical ion–cyclotron-resonance-heating

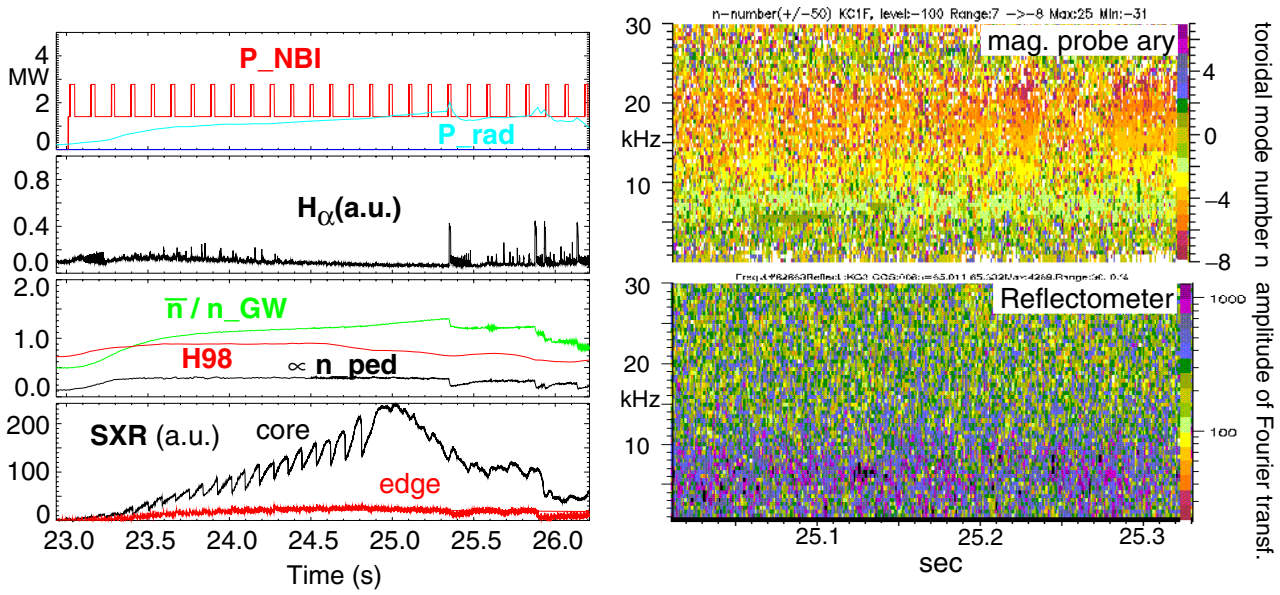

Figure 4. JET pulse 62663, $I_p = 0.68$ MA, $B_t = 0.94$ T, $q_{95} = 4.2$, aimed to be dimensionless identical to an Alcator C-mod EDA H-mode plasma. The figures to the right show the toroidal mode number analysis (negative numbers correspond to the electron diamagnetic drift direction) and density fluctuations measured in the steep gradient region with the reflectometer (34 GHz $\hat{=}1.4 \times 10^{19}$ m^{-3}).

(ICRH) and the ratio of the frequencies of dimensionless identical MHD-modes. It should be noted that the scalings can be violated if atomic physics or effects on the scale of the Debye length play an important role. Since the H-mode pedestal region is most affected by ELMs, the above mentioned dimensionless parameters should be matched in this region for comparison of the ELM behaviour. A source of ambiguity is usually the additional heating since NBI heating clearly involves atomic physics, and scaled ICRH frequencies may not be available. Also fuelling by wall recycling and gas puff does not fulfil the scaling requirement (i.e. the radial width of the particle-source profile does not scale with the major radius). Earlier pedestal dimensionless identity experiments showed that, for example, the L/H threshold [19] in JET and ASDEX Upgrade can be well scaled using the same values of ρ^*, ν^*, β, but not between ASDEX Upgrade and Alcator C-mod [20] hindering similar EDA-dimensionless-identity experiments such as those reported below for JET and Alcator C-mod.

3.1. Pedestal dimensionless identity to EDA-H-mode

The EDA-H-mode in Alcator C-mod is found above certain thresholds in δ, q_{95} and the pedestal density n_{ped}, and shows good H-mode confinement close to the (non-steady-state) ELM-free H-mode [8]. It is characterized by continuous MHD activity and density fluctuations between 60 and 120 kHz of rather narrow band width, located in the steep gradient region. These fluctuations are called the quasi-coherent mode (QCM). At higher pedestal temperatures T_{ped}, a transition to a grassy ELM regime is observed and the edge MHD frequency drops and becomes broadband (see, e.g. figure 4 in [8], where the grassy ELM MHD is observed in the whole frequency range between the original QCM and zero). It should be noted that the term 'grassy ELMs' is used on various machines for small ELMs which are neither type-I nor type-III. This does not mean that the grassy ELMs on different machines are necessarily the 'same thing'. For example, the grassy ELMs on Alcator C-mod occur in a collisionality range close to the type-II ELMs of ASDEX Upgrade but significantly higher than the grassy ELMs in JT-60U, which are discussed in section 4. Still, in this paper we use the original names given to the specific small ELM regimes in the original publications. After some iterations, a very good shape match between JET and Alcator C-mod was achieved (figure 3). The reference Alcator C-mod discharge shows the usual EDA behaviour. The experiments are described in detail in [15, 16]. The main difficulty in JET is the diagnosis of the edge pedestal as the JET diagnostic set was not designed to operate in this operational range ($I_p = 0.65$ MA, $B_t = 0.9$ T). Therefore, an uncertainty on the pedestal pressure of about 50% remained, spanning the scaled value from Alcator C-mod, essentially due to uncertainties in the pedestal temperature [16]. Nevertheless, in the steep gradient zone at the plasma edge, good agreement of $\nabla n_e, \nabla T_e$ with the scaled values of Alcator C-mod was observed. It remains uncertain to what extent dimensionless identical plasmas have been achieved. The error bar of the pedestal temperature in these low-current JET-plasmas even includes the scaled T_{ped}-threshold of Alcator C-mod, which separates EDA and grassy-ELM behaviour. Additionally, the plasma behaviour depends crucially on small variations of the lower triangularity and on the heating method, which was either NBI or 2nd harmonic hydrogen minority heating with ICRH, in contrast to 1st harmonic minority heating at Alcator C-mod (i.e. ICRH frequencies could not be matched according to dimensionless scaling). No controlled EDA modes have been found at JET, but phases with a steady pedestal were observed for several τ_E (up to 1 s). Magnetic and density fluctuation patterns observed with pick-up coils and a reflectometer are variable in terms of

strength and bandwidth. Often the fluctuations are enhanced in the 10–20 kHz range. They rotate in the direction of the electron diamagnetic drift as observed for the QCM in Alcator C-mod. The bandwidth Δf of these enhanced fluctuations in JET is occasionally lower than 1 kHz. In such cases at least two harmonics of a base frequency of 10–15 kHz are observed (higher ones are very weak) [15, 16]. According to the dimensionless identity scaling, this frequency does correspond to the frequency range of 60–90 kHz at Alcator C-mod, which is within the frequency range of the QCM. Nevertheless, multiple harmonics are never observed with this shape at Alcator C-mod so that observations on both machines do not exactly match.

In JET these phases without ELMs and with constant $n_{\mathrm{ped}}, T_{\mathrm{ped}}$ are observed with NBI as well as with ICR. With ICRH, fluctuation patterns with a band width comparable to the QCM have been observed [15, 16]. A pure NBI-heated case is shown in figure 4, which shows one of the longest phases with steady pedestal conditions. Under these conditions edge density fluctuations are strongest in the upper half of the steep gradient zone, whereas in Alcator C-mod they are found in the lower half. With ICRH as well as with NBI, an increase in radiation leads to a transition to type-III ELMs with poorer confinement. The increase in radiation is observed simultaneously with a central peaking of the density profile. This recalls observations in DIII-D [21], ASDEX Upgrade [22], Alcator C-mod [23] and JET [24], in which a slow central density peaking has been observed for broad or off-axis peaked profiles of auxillary heating. Without further analysis it remains a speculation that similar effects could play a role in this case: as mentioned above, we know that the available auxillary heating schemes violate the dimensionless scaling approach. In H-modes, due to the strong density pedestal, NBI heating (as used in JET) always results in a much broader heating profile than central 1st harmonic ICR minority heating (as used in Alcator C-mod). Also for the 2nd harmonic ICR minority heating in JET, one may speculate that poorer single pass absorption and possibly additional impurity resonances at the plasma edge do broaden the heating profile. It remains to be verified that these differences in the heating profiles are really the reason for the observed differences in the central density profile evolution.

3.2. Dimensionless identity approach for type-II ELMs as in ASDEX Upgrade

In [3], three criteria were introduced for the characterization of type-II ELMs in ASDEX Upgrade: good H-mode confinement, quasi-continuous heat flux to divertor as measured by the infrared cameras (IR) and broadband fluctuations in density and magnetics in the steep gradient zone of the edge pedestal ranging from 20 to 40 kHz. Type-II ELMs are observed in QDN configurations with $q_{95} > 3.5$–4.0 in a narrow density band just below the transition to type-III ELMs. Steady state phases with pure type-II ELMs are only observed when q_{95} is above a threshold value which varies between 3.5 and 4.0, depending on plasma shape and β. As described in [3], a reduction of q_{95} below the threshold leads to a mixture with type-I ELMs, and the bandwidth of the inter-ELM fluctuations is reduced. Under these conditions the fluctuations occur in

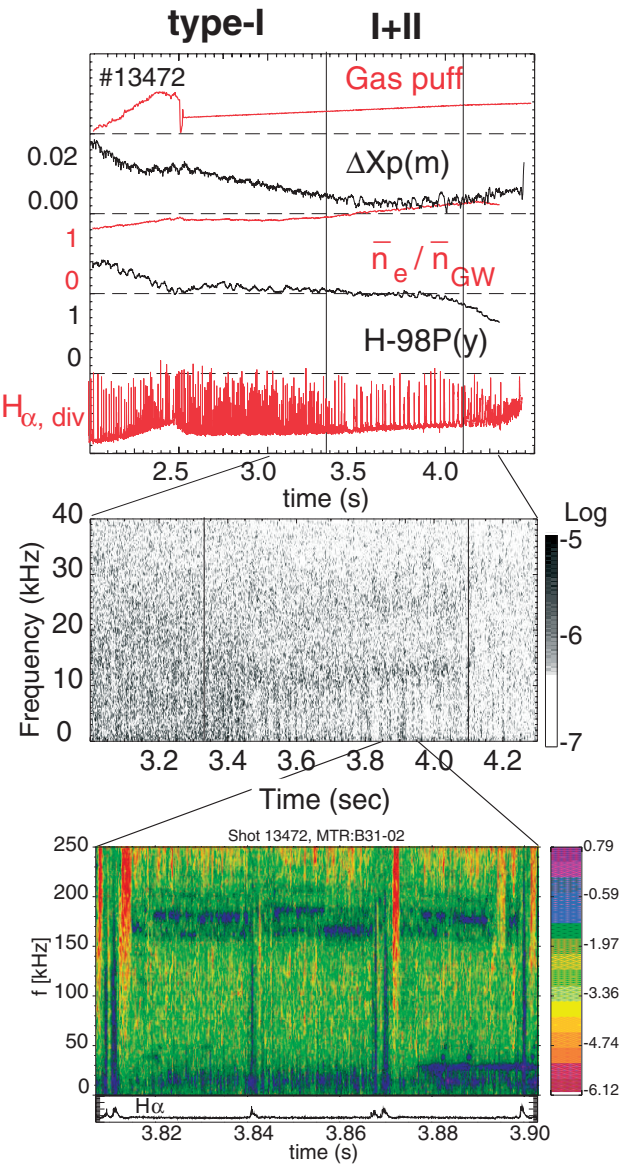

Figure 5. ASDEX Upgrade pulse 13472 0.8 MA, 2.0 T, $q_{95} = 3.9$, (see also [3]), corresponding to a mixed type-I/II phase. (ΔXp quantifies the closeness to a DN configuration. It denotes the distance of the inner separatrix with the lower x-point to the outer separatrix with the upper x-point measured at the outer midplane.) Middle: density fluctuation as seen by a reflectometer channel in the steep gradient region close to the pedestal top. Bottom: spectrogram of a magnetic signal together with an H_α trace from the outer divertor.

quite regular bursts ($\approx$ 0.5–1 kHz). Such a phase has been revisited for comparisons in this paper. The result is shown in figure 5 (and as a black curve in the right part of figure 6, which shows the peaks in the reflectometer spectrum more clearly). The highly localized reflectometer measurement shows two bands around 13 and 25 kHz during the mixed I/II phase whereas the MHD is more broadband in between 10 and 30 kHz. This MHD structure is sharp enough to determine its mode number, yielding $n \leqslant 4$ and $m \geqslant 12$, again in the direction of the electron diamagnetic drift. The MHD fluctuations between 150 and 200 kHz had been overlooked

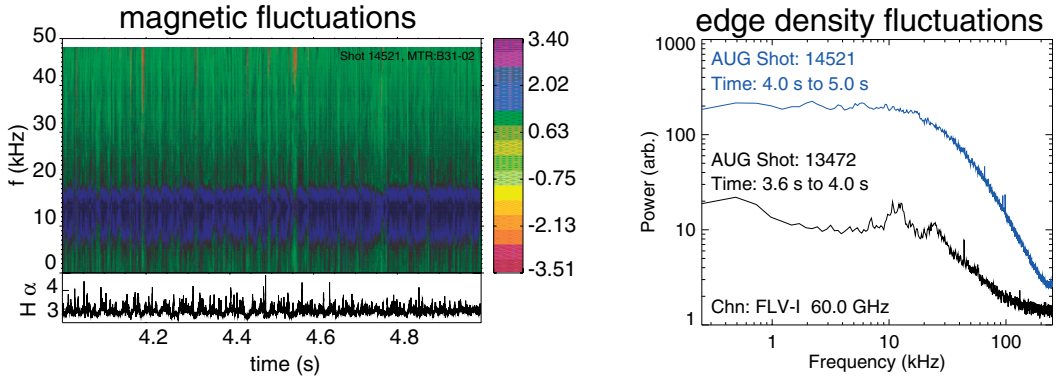

Figure 6. Fluctuation data for ASDEX Upgrade pulse 14521 0.8 MA, 1.7 T, $q_{95} = 3.5$, (see also [4]). Compared to figure 5 the discharge has twice as much heating power, 20% less density, same H-factor and therefore significantly higher temperatures and β_{pol} ($\approx$1.7) as well as significantly lower pedestal collisionality ($\nu^*_{\mathrm{ped}} \approx 0.6$). The strong MHD between 8 and 18 kHz is due to central fishbone and (1,1)-activity. Apart from this frequency range, no enhanced frequency band is observed. Also the reflectometer does not show any frequency bands with enhanced fluctuations in contrast to pulse 13472 from figure 5. For better comparison also the spectrum of the edge density fluctuations of pulse 13472 is shown. The location of the reflectometer measurement is not exactly the same, since #13472 has a pedestal density which is about 20% higher than #14521. Still, both measurements are located in the upper half of the steep gradient zone. For #14521 the location is closer to the pedestal top.

earlier, but they are present in all type-II phases published in [3] and disappear at transitions to type-III ELMs. The mode numbers are in this case $n = 5$–7, $m \geqslant 12$, electron direction. More recent type-II experiments show that the MHD/reflectometer footprint are not found at higher power and/or strong ICRH (>3 MW) although the other two criteria still hold. As an example, figure 6 shows the magnetic spectrogram and the spectrum of edge-density-fluctuation for an improved H-mode with high β_{N} and type-II ELMs at $q_{95} = 3.5$ as described in [4]. This does not necessarily mean that the modes are not present; they may be hidden by the significantly higher amplitude of all frequencies in the analysed frequency range or the radial location of the density fluctuation measurement may have changed slightly due to changes in the density pedestal-profile.

Due to differences in the sets of poloidal-field coils a close shape match of the high-δ ASDEX Upgrade equilibria was impossible at JET, so that a QDN configuration with the same average δ has been chosen as shown in figure 7. To reduce the diagnostic problems at very low currents discussed in the previous section, the plasma current in JET ($I_{\mathrm{p}} = 0.9$ MA, $B_{\mathrm{t}} = 1.2$ T, $q_{95} = 4.1$) was chosen to correspond to a 1 MA ASDEX Upgrade discharge although only 0.8 MA were run at ASDEX Upgrade with the high-δ shape used in [3]. Figure 8 shows that indeed long phases without ELMs and steady pedestal parameters have been achieved. As in the case of the EDA identity (figure 4) the central density slowly rises, terminated by the loss of sawteeth and a radiation collapse. In the previous section we speculated that this was due to the broader heat deposition profile in JET as compared to the central ICR in Alcator C-mod, in accordance with observations on several tokamaks. This explanation does not hold for the density peaking in the JET discharges dimensionally similar to ASDEX Upgrade, since the profile of the NBI heating power in ASDEX Upgrade is almost flat, but in the dimensionless identical JET plasma the heating profile is peaked centrally with the maximum around $\rho = 0.2$. Since the major mismatches in the dimensionless scaling are the heat flux

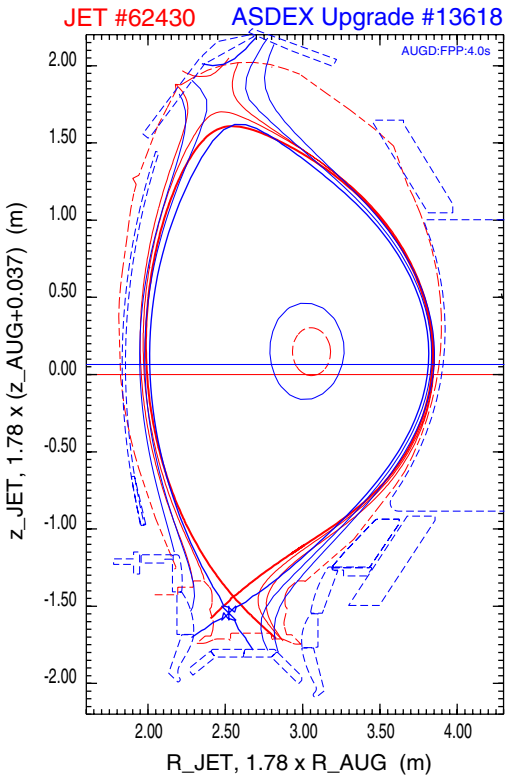

Figure 7. Scaled shapes used for the JET/ASDEX Upgrade type-II identity experiments. Some discrepancies could not be avoided, especially in the outer lower region and the inner upper region. Aspect ratio, elongation and average delta are well matched. The JET equilibrium is a prediction using the PROTEUS code, with the actual coil currents and plasma beta. The ASDEX Upgrade equilibrium is reconstructed from the magnetic data using function parametrization.

profiles and the shapes in the vicinity of the upper and lower x-points one may speculate about other possible reasons related to these quantities: the most striking difference of the NBI heating in both machines is that in JET about 80% of the

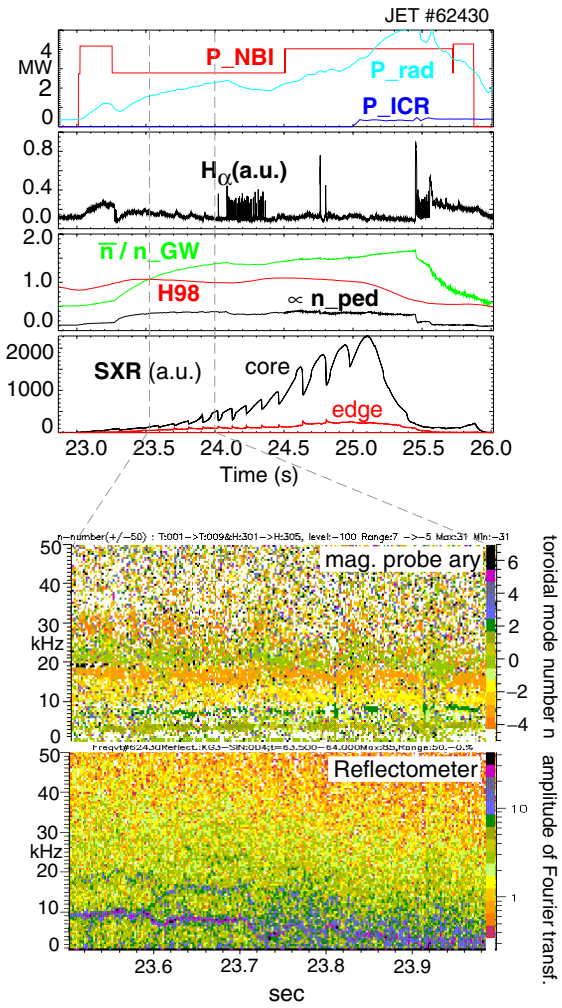

Figure 8. JET pulse 62430, $I_p = 0.86$ MA, $B_t = 1.15$ T, $q_{95} = 4.1$, aimed to be dimensionlessly identical to ASDEX Upgrade type-II H-modes. The lower part of the figure shows the toroidal mode number analysis (negative numbers correspond to the electron diamagnetic drift direction) and density fluctuations measured in the steep gradient region with the reflectometer (34 GHz $\hat{=}1.4 \times 10^{19}$ m^{-3}).

heating goes to the electrons, whereas in ASDEX Upgrade this fraction is approximately 50%. It remains an open question if this difference relates to the different behaviour of the central density. In the JET/ASDEX Upgrade case also the mismatch in upper triangularity may be responsible for the behaviour, since it is found on ASDEX Upgrade that higher upper triangularity favours the occurrence of slow density peaking and the mismatch of the shapes is indeed such that the JET plasma has a higher upper triangularity as compared to the ASDEX Upgrade plasma. Also, the steady profiles in ASDEX Upgrade are only obtained if $q_{95} \geqslant 3.8$; below this value also in ASDEX Upgrade the slow central density peaking is observed. Such a case is shown in figure 5 (the pedestal density is constant from 3.5 to 4.2 s), indicating that small differences in the discharge parameters can indeed trigger an unstable behaviour of the central density.

In the following, the fluctuations observed in JET in the region of the steady H-mode pedestal are discussed. Figure 8 shows the spectrogram of a reflectometer channel in the steep gradient region and the MHD mode number analysis for JET pulse 62430. Two sharp bands are observed with the reflectometer at approximately 8 and 15 kHz, rather close to what is expected from the dimensionless identity scaling of frequencies from ASDEX Upgrade to JET as described in the introduction to section 3 (see figure 5, scaling factor $(a_{AUG}/a_{JET})^{1.25} \approx 0.5$, using $(a_{AUG}/a_{JET}) = 1.78$ from figure 7). As in ASDEX Upgrade the MHD fluctuations are less sharp and again they move in the direction of the electron drift. The n-number of the mode between 15 and 20 kHz is close to 4, the minimum m-number is estimated to be 7, a lower limit depending on the present set of pick-up coils. These numbers also relate well to the findings on ASDEX Upgrade ($n = 4, m > 12$). After 23.7 s the bandwidth of the modes measured with the reflectometer increases and the frequency drops in contrast to the MHD analysis. Due to the strong radial localization of the reflectometer this could be due to the still slightly increasing edge density, shifting the location of the measurement further towards the separatrix and possibly away from the mode. In any case, this example shows that bandwidth and frequency of the observation are subject to a significant variation. We also note that the upper frequency bands observed in ASDEX Upgrade (see figure 5) should appear around 100 kHz in JET according to the scaling. Figure 9 shows a discharge where the small ELM phase is shorter but with magnetic data at a higher sampling frequency. Indeed, a weak band is observed in the magnetics at 110 kHz, rotating in the expected electron drift direction, with $n \approx 2$ which is lower than in ASDEX Upgrade. After having successfully established the scenario at JET using the dimensionless identity approach, the intention was to increase plasma current and magnetic field. The plasma current was increased from 0.9 to 1.2 MA and 1.5 MA at fixed q_{95}. Figure 10 shows that for 1.2 MA only mixed type-I/II phases were obtained with the type-II phases lasting up to 0.3 s. At 1.5 MA only high frequent type-I ELMy H-modes were found (see figure in [12]) resembling the behaviour observed at $q_{95} \approx 4$ at higher plasma currents as mentioned in section 2. Although the search at the higher currents was rather coarse due to time limitations, the failure indicates that it is more difficult if not impossible to get the pure type-II phases with increasing current, especially since the low current scenario was obtained in three campaigns during 2003 in a quite straightforward manner, using a coarse gas scan.

4. The high β_{pol} grassy ELM scheme of JT-60U applied to JET and ASDEX Upgrade

Another small ELM regime with good confinement is the grassy ELM regime observed in JT-60U. The most recent publication is [6]. As reported by JT-60U [5], a high value of β_{pol} facilitates operation with grassy ELMs most probably due to the stabilizing effect of a strong Shafranov-shift [25, 26]. The regime is observed as β_{pol} exceeds a value of 1.4–2.0 depending on q_{95} and δ. High values of the latter two quantities favour the occurrence of the grassy ELM regime. Typical values are $\beta_{pol} \geqslant 1.6$ and $q_{95} \approx 6$ for $\delta \approx 0.5$. The grassy ELM regime can be extended towards lower q_{95} ($q_{95} < 4$), by increasing the triangularity up to $\delta \approx 0.6$ [25]. Usually

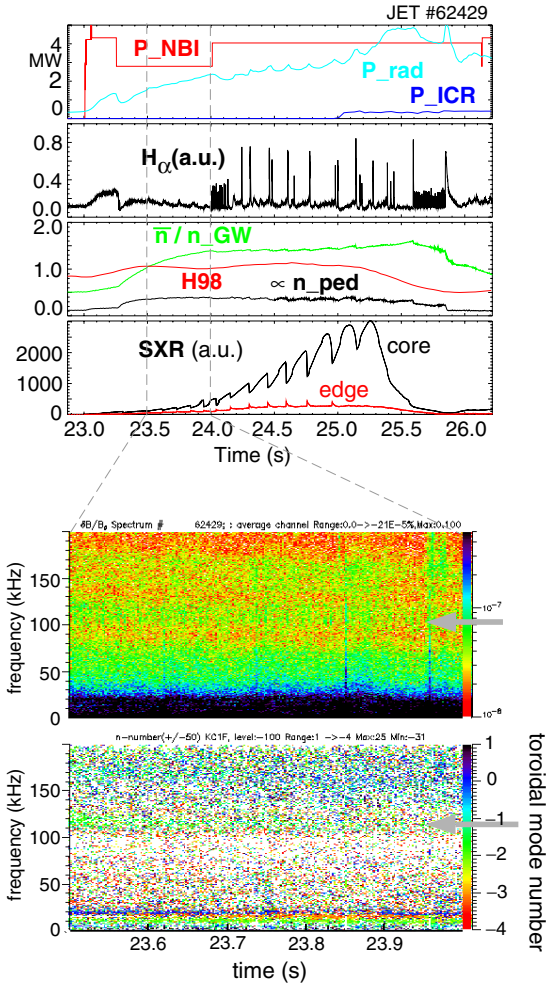

Figure 9. JET pulse 62429, $I_p = 0.86$ MA, $B_t = 1.15$ T, $q_{95} = 4.1$, with similar conditions as figure 8, but faster magnetics available. The lower part of the figure shows spectrogram and toroidal mode number analysis (negative numbers correspond to the electron diamagnetic drift direction) of magnetic data.

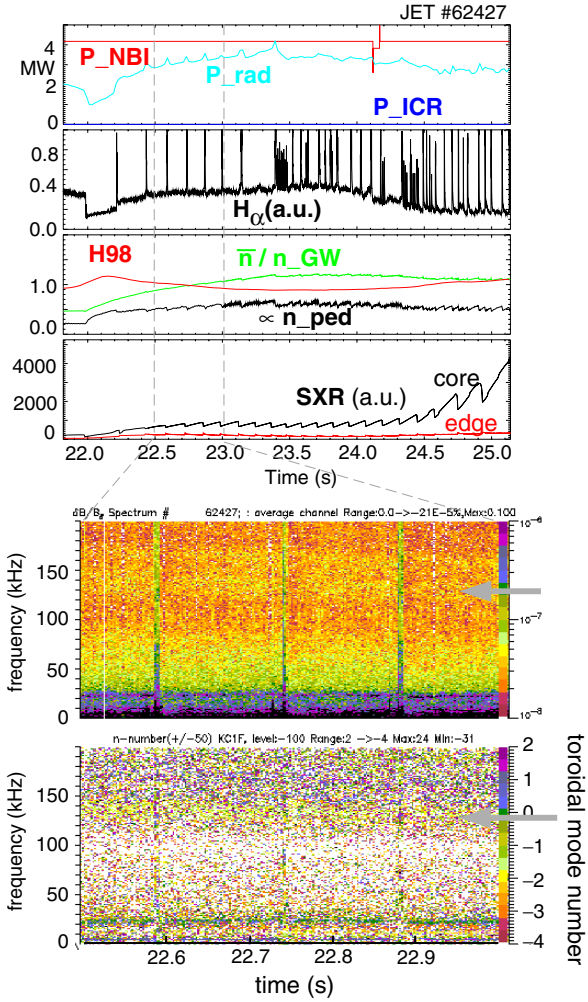

Figure 10. JET pulse 62427, $I_p = 1.2$ MA, $B_t = 1.6$ T, $q_{95} = 4.1$. The figures to the right bottom show spectrogram and toroidal mode number analysis (negative numbers correspond to the electron diamagnetic drift direction) of magnetic data. In this discharge the gas puff is constant up to 23.5 s and is then ramped down linearly to zero (24.0 s).

the regime is operated with an internal transport barrier using early heating to avoid the occurrence of sawteeth. Figure 11 shows time traces of JT-60U pulse E42857, which has been used to compare the magnetic fluctuation signals with those obtained at JET, as discussed below. The grassy ELM regime has significantly lower collisionality $\nu^*_{ee} \approx 0.1$ as compared to the high density small ELM regimes discussed above which have $2 \geqslant \nu^*_{ee} \geqslant 0.5$. This triggered experiments to transfer it to JET and ASDEX Upgrade. These experiments were not meant to match the JT-60U plasmas in the strict sense of a dimensionless identity experiment, but the key ingredients high β_{pol}, high δ and high q_{95} have been used for plasmas that already showed signs of mixed type-I/II ELMs at lower values of q_{95} and β_{pol}.

4.1. High β_{pol} grassy ELM experiments at JET

In JET, the shape developed for the identity experiment with ASDEX Upgrade was also used for the high β_{pol} experiment, with somewhat increased plasma current (1.2–1.5 MA) but strongly increased magnetic field (2.7 T) and plasma heating (17–23 MW, i.e. all power available on the day). This also means that the configuration was close to DN. Above a β_{pol}-value of 1.8 only very small ELMs are observed [12]. The energy carried by them is so small that it cannot be quantified (<5% of W_{ped}) in contrast to the type-I ELMs at lower β_{pol} each of which carry 15% or more of W_{ped}. The magnetic spectrogram and the fast D_α trace of such a JET-grassy-ELM phase are shown in figure 12. They are compared to a grassy ELM phase of JT-60U discharge E42857 (figure 11). The spectrograms look similar. In particular there are no modes seen in the range of a few 10 kHz or at even higher frequencies. Such high values of β_{pol} could only be achieved at JET at $I_p = 1.2$ MA due to limitations in heating power. There is no evidence that this is a physics-based limit. In parallel to these experiments another set of high β_{pol} discharges has been run at JET to study the effect of the high β_{pol} on the core transport together with a flat q-profile and consequently lower l_i and higher edge currents, using lower hybrid pre-heating and early main heating. Further

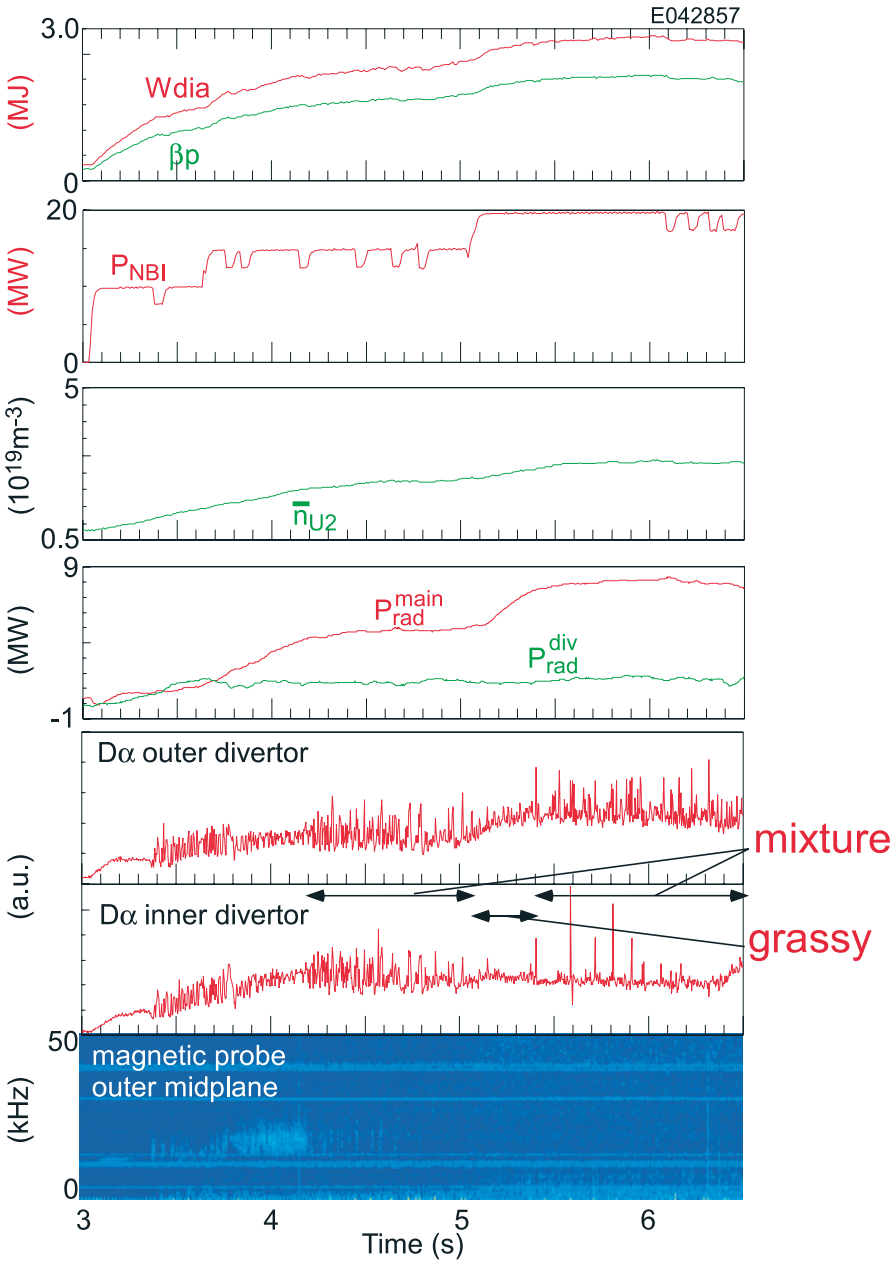

Figure 11. JT-60U pulse E42857, $I_p = 1.0$ MA, $B_t = 3.6$ T, $q_{95} = 6.4$, $\beta_{pol} = 2.0$, has pure grassy ELM phase between 5.1 and 5.4 s.

differences are that the plasma shape was clearly a lower SN shape and that the pedestal collisionality was about 50% lower. Interestingly, no grassy ELMs were observed even at $\beta_{pol} = 1.9$ [12]. Obviously the relative importance of the above-mentioned differences has to be separated by further experiments.

4.2. High β_{pol} grassy ELM experiments at ASDEX Upgrade

The high β_{pol} strategy has also been tried recently on ASDEX Upgrade. Pure grassy ELMs were found with a configuration close to DN [27]. The plasma shape is close to the original type-II shape [3], with stronger heating (14 MW) similar to the improved H-modes which can be integrated with type-II ELMs [4]. In contrast to these earlier experiments, q_{95} is increased to ≈7 to access the grassy ELM regime according to the operational boundaries determined at JT-60U. This is done by increasing B_t to 3 T keeping $I_p = 0.8$ MA. The resulting grassy ELM regime could indeed be accessed at lower densities as compared to the original type-II regime. ν^* is more than a factor 3 smaller than in the original type-II regime and similar to the value of 0.6 obtained in the above mentioned improved H-modes with small ELMs at lower q_{95}. The spectrogram of a magnetic pick-up probe is shown in the central part of figure 13. It is similar to what has been found on JT-60U and JET (figure 12), although the affected frequency region extends up to 10 kHz, perhaps due to the smaller machine size. For a very similar SN configuration only mixed type-I/grassy phases were obtained. In this case the magnetic fluctuations occur in the same frequency range but are correlated in time with the remaining type-I ELMs

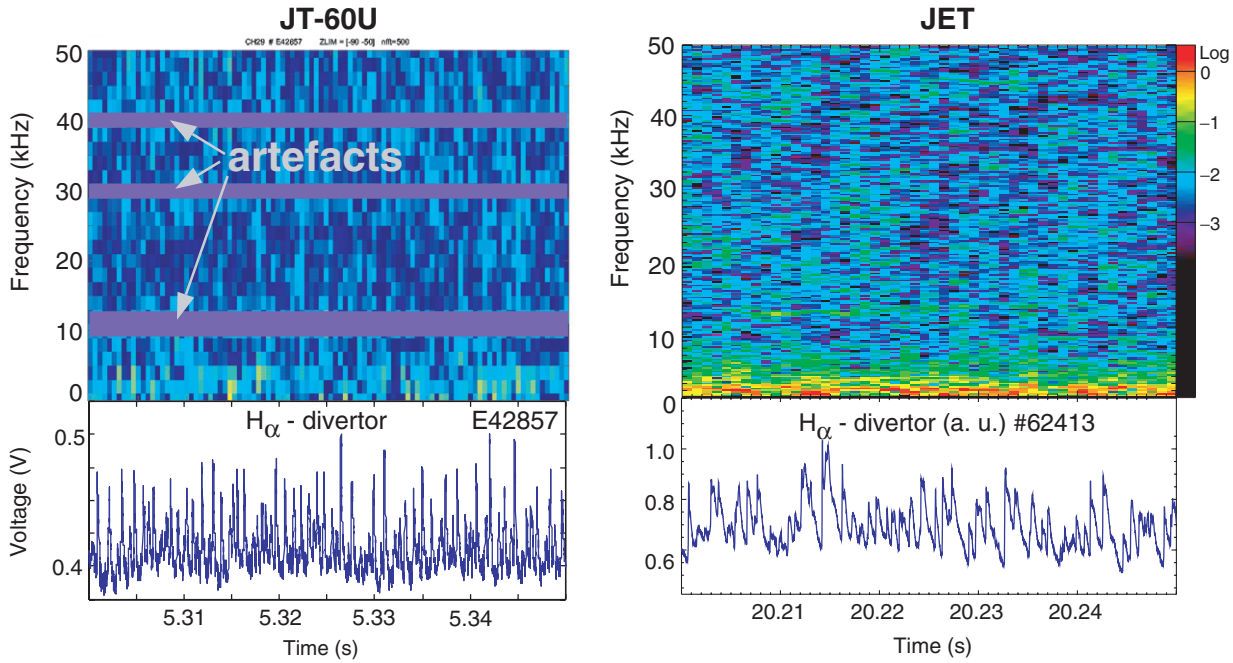

Figure 12. Magnetic spectrograms during grassy ELM phases. JT-60U pulse E42857: $I_p = 1.0$ MA, $B_t = 3.6$ T, $q_{95} = 6.4$, $P_{aux} \approx 20$ MW, $\beta_{pol} = 2.0$, JET pulse 62413: $I_p = 1.2$ MA, $B_t = 2.7$ T, $q_{95} = 6.9$, $P_{aux} \approx 23$ MW, $\beta_{pol} = 1.8$.

(vertical bars in the upper part of figure 13). Infrared divertor thermography shows high bursty H_α-correlated heat flux on the outer plate only for the SN case whereas for the DN case the heat flux remains steady at the inter-ELM level of the SN case. It is not clear in how far these high-q_{95} grassy ELMs are different from the earlier type-II ELMs, inasmuch as there are differences in the MHD spectra. As already mentioned, type-II ELMs are also found in improved H-modes [4]. These plasmas have $q_{95} = 3.5$ lower than the earlier type-II plasmas but a $\beta_{pol} \approx 1.6$ close to that of the grassy ELMs at high q_{95}. As shown in figure 6, they do not show enhanced fluctuations below 5 kHz nor the modes at a few 10 kHz. The edge density fluctuation spectra for the high q_{95}-case grassy ELMs (figure 13 bottom) and the low q_{95}-case so far identified as type-II ELMs (figure 6 right) are very similar, and it remains to be verified if there is a continuous transition between both, and at which value of q_{95} the magnetic fluctuations at a few kilohertz set in.

5. Conclusions

H-modes with an edge behaviour reminiscent of EDA, high density type-II ELMs and high β_{pol} grassy ELMs have been developed at JET, of which only the latter was fully controlled, whereas the others were limited by radiation collapses due to central density peaking. The operational regime is restricted to plasma currents below 1 MA for the pure type-II ELMs. The mixed type-I/II phases observed at JET earlier at 2.5 MA could also not be transferred to pure type-II phases by using either DN configurations or higher values of q_{95}. In dimensionless parameters, essentially ρ^* and ν^* decrease with increasing current. Although the change in ρ^* is larger, the change in ν^* is usually favoured as an explanation for this current scaling, since it directly influences the edge bootstrap current and therefore the stability of edge current driven peeling modes [28,29]. The plasmas which were meant to be dimensionlessly identical either to the EDA mode in Alcator C-mod or to the type-II ELMs of ASDEX Upgrade were very similar in terms of mode activity observed in the magnetic and reflectometer signals in JET, indicating a close relation between both phenomena. Nevertheless it must be noted that only part of this turbulence footprint matches the observations on Alcator C-mod and ASDEX Upgrade. A striking difference between both sets of experiments is that the EDA experiments were done in the same SN configuration which shows the mixed type-I/II ELMs at higher current whereas the type-II identity shots were done in a QDN configuration which is a pre-requisite for pure type-II ELMs in ASDEX Upgrade. An explanation for these contradictory findings could be that rather a quantity related to QDN, for example, the magnetic shear in the steep gradient region, is a crucial parameter. In the specific JET SN configuration it may be created by other moments of the shape. As mentioned above, the high β_{pol} plasmas in JET only showed pure grassy ELMs when close to DN, but other parameters, especially the current-density at the plasma edge, were changed as well. These effects can only be separated in future experiments.

In JET, for the high β_{pol} scheme the current was limited to 1.2 MA, but this is due to a limit in additional heating power. The high β_{pol} discharges on JET and ASDEX Upgrade showed similar fluctuations in the MHD spectrogram as observed in JT-60U. Nevertheless, they were at least a factor 4 higher in ν^* than those observed in JT-60U ($\nu^*_{\text{JT-60U}} \approx 0.1$), whereas in JET the low l_i discharges with high β_{pol} reached approximately the JT-60U collisionality values but did not show grassy ELMs. This is especially striking since the JT-60U discharges are also usually operated with early heating. An experimental separation of the relevance of ν^*, l_i, q_{95} and closeness to DN

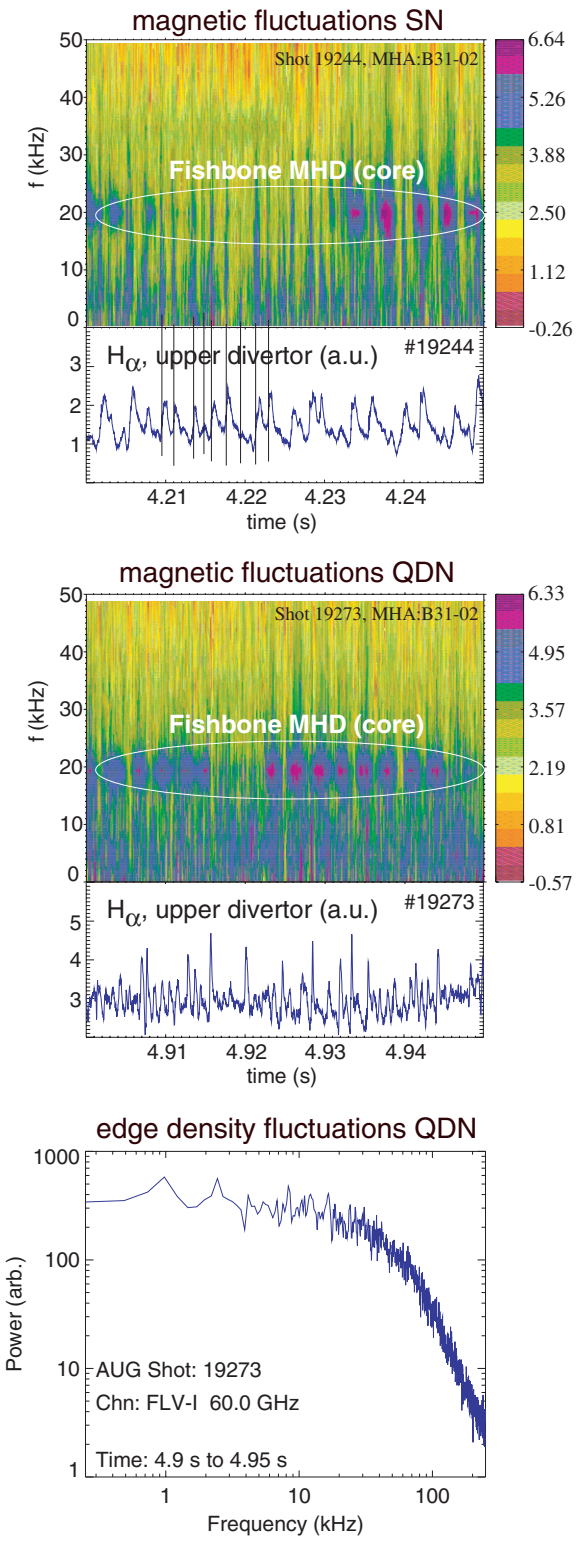

Figure 13. Magnetic spectrograms and H_α traces for two ASDEX Upgrade pulses differing only by the closeness of the second (upper) x-point to the separatrix, i.e. lower SN (#19244, top) and QDN (#19273, middle): $I_p = 0.8$ MA, $B_t = 3$ T, $q_{95} \approx 6.2$, $P_{aux} \approx 18$ MW, $\beta_{pol} = 1.8$. At the bottom the spectrum of the density fluctuations is shown for the QDN case, as obtained from reflectometer data from the upper half of the steep gradient zone.

for the appearance of grassy ELMs at high β_{pol} in JET is still outstanding. In view of a future reactor plasma, our results suggest that only the high β_{pol} scheme may be extrapolatable, but means have to be found to run it at lower values of q_{95}, as was possible on JT-60U using very strong shaping ($\delta \approx 0.6$) [25].

References

[1] Loarte A. *et al* 2004 *Phys. Plasmas* **11** 2668
[2] ITER Physics Basis 1999 *Nucl. Fusion* **39** 2137, for confinement scaling IPB98(y, 2) see p 2204
[3] Stober J. *et al* 2001 *Nucl. Fusion* **41** 1123
[4] Sips A.C.C. *et al* 2002 *Plasma Phys. Control. Fusion* **44** A151
[5] Kamada Y. *et al* 2000 *Plasma Phys. Control. Fusion* **42** A247
[6] Oyama N. *et al* 2005 *Nucl. Fusion* **45** 871–81
[7] Greenwald M. *et al* 1999 *Phys. Plasmas* **6** 1943
[8] Mossessian D.A. *et al* 2003 *Plasma Phys.* **10** 1720
[9] Suttrop W. *et al* 2005 *Nucl. Fusion* **45** 721–30
[10] Saibene G. *et al* 2002 *Plasma Phys. Control. Fusion* **44** 1769
[11] Sartori R. *et al* 2005 *Proc. 20th IAEA Conf. on Fusion Energy (Vilamoura, Portugal, November 2004)* vol IAEA-CSP-25/CD (Vienna: IAEA) CD–ROM file EX/6–3 and http://www–naweb.iaea.org/napc/physics/fec/fec2004/datasets/index.html
[12] Saibene G. *et al* 2005 *Nucl. Fusion* **45** 297
[13] Perez C.P. *et al* 2004 *Plasma Phys. Control. Fusion* **46** 61
[14] Smeulders P. *et al* 1999 *Plasma Phys. Control. Fusion* **41** 1303
[15] Maddison G.P. *et al* 2003 EDA H-mode pedestal identity studies on JET and Alcator C-Mod *Proc. 30th EPS Conf. on Controlled Fusion and Plasma Physics (St Petersburg, 2003)* (*Europhysics Conf. Abstracts*) vol 27A, ed R. Koch and S. Lebedev (Geneva: EPS) P-1.109, (CD-ROM)
[16] Mossessian D.A. *et al* H-mode pedestal physics studies in local dimensionless identity experiments *Proc. 30th EPS Conf. on Controlled Fusion and Plasma Physics (St Petersburg, 2003)* (*Europhysics Conf. Abstracts*) vol 27A, ed R. Koch and S. Lebedev (Geneva: EPS) P-3.182, (CD-ROM)
[17] Kadomtsev B.B 1975 *Sov. J. Plasma Phys.* **1** 295
[18] Connor J.W. and Taylor J.B 1977 *Nucl. Fusion* **17** 1047
[19] Suttrop W. *et al* 2003 *Fusion Sci. Technol.* **44** 636
[20] Suttrop W.A. *et al* 2002 Parameter similarity studies in JET, ASDEX Upgrade and ALCATOR C-Mod *Proc. 19th IAEA Conf. on Fusion Energy (Lyon, France, October 2002)* vol IAEA-CSP-19/CD (Vienna: IAEA) CD–ROM file EX/P5–07 and http://www.iaea.org/programmes/ripc/physics/fec2002/html/fec2002.htm
[21] Mahdavi M.A. *et al* 2002 *Nucl. Fusion* **42** 52
[22] Stober J. *et al* 2003 *Nucl. Fusion* **43** 1265
[23] Rice J.E. *et al* 2003 *Nucl. Fusion* **43** 781
[24] Valovic M. *et al* 2002 *Plasma Phys. Control. Fusion* **44** 1911
[25] Kamada Y. *et al* 2002 *Plasma Phys. Control. Fusion* **44** A279
[26] Saarelma S. and Günter S. 2004 *Plasma Phys. Control. Fusion* **46** 1259
[27] Horton L.D. *et al* 2004 *Max-Planck-Institut für Plasmaphysik* Garching, Germany, private communication
[28] Saarelma S. *et al* 2003 *Nucl. Fusion* **43** 262
[29] Lönnroth J.-S. *et al* 2004 *Plasma Phys. Control. Fusion* **46** 767